Symbolic dynamics analysis of nonstationary data from a model of a magnetic system with solitons

T. Buchner* and J. J. Żebrowski†
Institute of Physics, Warsaw University of Technology, ul.Koszykowa 75, 00-662 Warszawa, Poland
(Received 6 July 1998; revised manuscript received 10 March 1999)

The probability distribution of a complexity measure is used to characterize chaotic states: an estimator of the algorithmic complexity of a time series of symbolic words is calculated within a fixed length time window, which sweeps through the time series analyzed. The words are derived through a symbolic dynamics scheme applied in an *m*-dimensional delay coordinate space. Time intervals instead of the variables of the system are used. The chaotic states of a model of a magnetic domain wall are characterized better by the methods presented than with the use of fractal dimensions and new intermittent states of the system were easily identified. Using an artificial nonstationary signal composed of different chaotic states of the Bloch wall as a test for chaos-chaos intermittency we demonstrate that the method developed is suitable for the detection and characterization of intermittency. It is also shown that nonstationarity in the form of a slow monotonic drift in the control parameter may extend the stability range of periodic states of the spatially extended system studied—a trackinglike phenomenon. [S1063-651X(99)11510-1]

PACS number(s): 05.45.−a, 75.10.Hk, 75.60.Ch

I. INTRODUCTION

To quantify the properties of chaotic states of nonlinear dynamical systems, complexity measures such as fractal dimensions, Liapunov exponents, and various types of entropy [1] are often applied. The major drawback of many complexity measures used to characterize the properties of chaotic states is that they are defined for trajectories of infinite lengths. This is because the dynamical systems analyzed are assumed to be ergodic [2]. One way of characterizing a system, which may not be ergodic, is to study the probability distribution of the given complexity measure. Such an approach was implemented in [3] where the probability distribution of the local Liapunov exponents of a classical cluster Ar_3, whose ergodicity depends on its energy, was analyzed for a set of increasing values of the lengths into which the trajectory of the system was partitioned. Conclusions as to the properties of the states at different energy levels were drawn from the shape of the probability distributions of the local Liapunov exponents.

Ergodicity is questionable especially when nonstationarity of the system is expected. The aim of this paper is to show that complex chaotic states may be characterized by the probability distribution of a complexity measure calculated within a fixed length time window, which sweeps through the time series analyzed. We show that the method developed is equally well suited to analyze nonstationary states of chaotic systems as well as intermittency. The complexity measures mentioned earlier typically quantify the statistical properties of the state analyzed. Instead, symbolic dynamics [4] may be applied [5–9] to detect the sequential order in the signal, ignoring information about the details of the trajectory in phase space. As the complexity measure in the symbolic dynamics, we use an estimator of the algorithmic complexity [10] of a time series of symbolic words. The words are derived through a symbolic dynamics scheme defined in such a way that it maps a trajectory from an *m*-dimensional delay coordinate space into the *m*-dimensional symbol space (multidimensional coding [6,8,9]). We verify the usefulness of this approach to the analysis of nonstationary data.

Searching for the kind of data, which may be relatively easily extracted from a time series, we discuss the use of time intervals between zero crossings of the variables of the system studied and compare the results with the analysis of the successive extrema of the variables of the system. We show that the approach described is able to arrange in parameter space the chaotic states of a model of a spatially extended system with solitons—the Bloch magnetic domain wall [11–18]—according to their complexity. The states of the Bloch wall may be more precisely identified by time intervals than by using just the system variables. We demonstrate this by studying newly identified intermittency states associated with a symmetry breaking phenomenon. Forming an artificial nonstationary signal composed of different chaotic states of the Bloch wall, we show that the method developed is able to analyze chaos-chaos intermittency, i.e., identify in the signal the phases with a different level of complexity and precisely identify moments of rapid switching between these phases. Thus, the method is also suitable for the analysis of nonstationary signals. Next, we analyze the effect of a slow monotonic drift in the control parameter (the drive field magnitude) on the dynamics of the Bloch wall and find that such a drift may stabilize some of its periodic states. The possible reasons for this effect are discussed.

II. THE MODEL

We analyzed the model of a spatially extended, micromagnetic system—a magnetic domain wall of the Bloch-type (Fig. 1). This system has been studied in the past in several

*Electronic address: buchner@if.pw.edu.pl
†Electronic address: zebra@if.pw.edu.pl

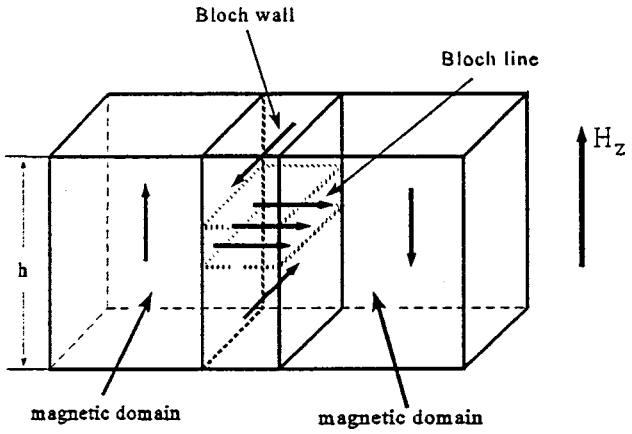

FIG. 1. Schematic of the Bloch magnetic domain wall in a thin film of uniaxial magnetic material of thickness h. The arrows inside the domain wall mark the direction of the magnetization. Within the Bloch wall and within the Bloch line only the central magnetization vectors are marked.

contexts [11–18]. It is described by a pair of nonlinear partial differential equations of motion, which can be derived from the Landau-Lifshitz-Gilbert equation [17,18]:

$$\dot{q} = \gamma\Delta\left[2\pi M \sin(2\varphi) - \frac{2A}{M}\frac{\partial^2\varphi}{\partial z^2}\right] + \alpha\Delta\dot{\varphi}, \tag{1}$$

$$\dot{\varphi} = \gamma\left[H_z + \frac{2A}{\Delta M}\frac{\partial^2 q}{\partial z^2}\right] - \alpha\frac{\dot{q}}{\Delta}, \tag{2}$$

where the z variable is perpendicular to the surface of the magnetic film in which the domain wall resides, $q(z,t)$ is the position of the wall, $\varphi(z,t)$ is the azimuthal angle between the magnetization vector and the wall surface, H_z is the spatially uniform and constant in time drive field, α is the phenomenological damping constant, γ is the gyromagnetic ratio, $4\pi M$ is the saturation magnetization, A is the exchange constant, and $\pi\Delta$ is the Bloch wall width. The azimuthal angle φ is given in radians while the position of the wall q is given in units of the wall width parameter Δ.

The model of the Bloch wall may only be analyzed by numerical means. Below we used the explicit finite difference scheme of [18] with the same time step as used there (0.05 ns). This scheme is extremely stable and, in the present study, has enabled us to calculate trajectories of the Bloch wall exceeding 163 μs in length, i.e., 3.26×10^6 numerical time steps. For initial conditions, we assumed that the wall is flat $[q(z,0)=0]$ and that all the magnetic moments lie in the plane of the wall $[\varphi(z,0)=0]$. As in [18] we assumed force-free boundary conditions neglecting the surface stray field.

$$\frac{\partial q}{\partial z} = 0,$$

$$\frac{\partial \varphi}{\partial z} = 0. \tag{3}$$

As the control parameters, the drive field magnitude H_z and the distance between the surfaces of the film, i.e., the height of the wall h were used. The latter does not enter explicitly into the equations of motion and affects the dynamics of our system through the number of spatial grid points used in the numerical integration with the distance between grid points fixed.

The initial conditions given above used with our model of the Bloch wall (Fig. 1) would result in the numerical equivalent of the well-known Walker model [19]: a spatially uniform precession in the azimuthal angle $\varphi(z,t)$ would last for ever. The motion of the wall would be either running—oscillatory or with a constant velocity—if the external drive field H_z is less than the Walker critical field H_w (a characteristic of the magnetic material [18,19]—here $H_w = 10.92$ Oe). The uniform precession mode is unstable, however. When $H_z > H_w$ and the symmetry of the system is broken (in our case by a 0.08% change of the drive field at an arbitrarily chosen, single spatial grid point for two time steps) coherent spacial structures—Bloch lines (Fig. 1)—are generated at drives above the Walker field [17,18]. The Bloch lines connect regions of magnetic moments at the energy minimum orientations at $\varphi = n\pi$, $n = 0, \pm1, \pm2, \pm3, \ldots$ and pass through the energy maximum located exactly in between, at $\varphi = n\pi/2$.

One or several of such coherent spatial structures are present during the motion of the Bloch wall in any one of the states studied below. Their number depends on the state but is, in general, greater when the height of the wall is increased. Soliton properties of the coherent spatial structures of the Bloch wall [17] are an important feature of the system. The soliton properties of the Bloch lines are retained, even though the system is dissipative, provided the drive field Hz is large enough to compensate for the dissipation [17]. The propagation of solitons along the Bloch wall of a finite height results in nonmonotonic correlations of the dynamics occurring at remote parts of the wall [20,21]. The fractal dimensions and the spatial distribution of the dimension along the wall height were calculated in Refs. [11,12]. In particular, it was found that the values of the fractal dimensions do not differ significantly for the different chaotic states (only by about 20%).

For the drive field H_z greater than the Walker field the specific mode of motion of the wall depends on a combination of control parameters: the drive field magnitude H_z and the height h of the wall. For the magnitude of the drive H_z set at 12 Oe, i.e., 1.08 Oe above the Walker field, depending on the height h of the wall, periodic or chaotic states of the wall with coherent spatial structures occur (see also [15,16,18]). These structures are confined to the variable $\varphi(z,t)$ while $q(z,t)$, i.e., the position of the wall, undergoes a vibration forced by the propagation of the Bloch line.

III. THE DATA

A. Data reduction methods

Studying spatially extended systems, described by partial differential equations we typically obtain a large amount of information, which needs to be reduced in order to be analyzed efficiently. The reduction must not distort or ignore any important information about the studied state. The method that has focused much attention recently is to use time intervals between characteristic events during the evolution of a dynamical system [22,23]. This type of time se-

ries, which seems to be natural for biomedical research [24,25], has not been widely used with physical models and systems so far [26].

The idea was applied in the following steps. First, the analysis was limited to the projection of the phase portrait to the midplane of the film. The phase portrait was constructed in the frame moving with the wall by subtracting at each time step the average wall position and the average azimuthal angle. Although the system is spatially extended, it has been shown before [15–18] that the projection of the phase portrait to the midplane is sufficient to distinguish between different states. The results below will be given for the variable $\varphi(t)$; however, similar results were also obtained for the wall position $q(t)$. Next, the time intervals t_φ between consecutive zero crossings in the positive direction were found for the chosen variable. All the time intervals t_φ form a one-dimensional time series in which each orbit (in fact, half of the orbit) length is represented by a single value. Local extrema, namely, the minima φ_s of the variable $\varphi(t)$ between zero crossings were also recorded. Time series of the extrema of a selected variable were used by Lorentz [27].

For each state, after all transients had died out, we calculated the data on 5000 zero crossings. The time span of our data was thus 163 μs. In a real magnetic film, the Bloch wall may not move for such a long time as it would interact with the other walls. The unphysical length of the data series was used to discuss the properties of the method developed here but we show below that the number of data required to distinguish between states is only a few tens of zero crossings.

B. Stationary chaotic states

For the purpose of this study the range of wall height from $h=3.5–6$ μm was examined with a step equal to 0.005 μm, which is of the order of changes of height accessible in a magnetic film produced by epitaxy. The specific height range was chosen because, for the material parameters used here, it has been shown earlier [15–18] which dynamical states exist for several values of the height of the wall and a drive field magnitude fixed at 12.0 Oe. Apart from two periodic states, a period-2 state existing in the range of h between 1.2–3.0 μm and a period-4 state identified earlier at $h=4.0$ μm, there exist chaotic states of which five were chosen: $C1$ ($h=3.5$ μm), $C2$ ($h=4.5$ μm), $C3$ ($h=5.0$ μm), $C4$ ($h=5.5$ μm), and $C5$ ($h=6.0$ μm). The details of the time evolution of the system and the phase portraits for these states have been published elsewhere [15–18]. It is also known that for the relatively low magnitude of the drive field used here and in the range of wall height between 3.0 and 5.0 μm only two coherent spacial structures (Bloch lines) propagate along $\varphi(z,t)$ [15,18]. The number of Bloch lines increases sharply and may change with the time for wall heights larger than 5.0 μm. As found below, in this range of the wall height the complexity of the states of the system increases rapidly with the system size.

C. Nonstationary time series

In order to verify the efficiency of the method presented in identifying transitions between states during nonstationarity, an artificial test time series was considered. The t_φ time series calculated for the states $C1$ and $C3$ were combined to form alternating segments of equal length in such a way that one segment was taken from one state and the next segment from the other. The segments taken from each state did not repeat and resulted from the natural evolution of the respective states. The length of each segment was 500 points and the length of the whole time series was 5000. The segments were normalized so as to have the same mean and variance. This test signal mimics a particularly vicious case of chaos-chaos intermittency [1,28] in which the different chaotic phases are difficult to distinguish.

A different type of nonstationarity studied was obtained by simulating a slow, steady increase of the drive field in the range from 20–35 Oe and the wall height fixed at $h=1.1$ μm. The properties of the wall for this set of parameters had not been studied earlier. (Here we present only the results for the range from 25.8–26.2 Oe. The results in the rest of the drive field range studied were similar). During the evolution of the system every 7000 ns, the drive field magnitude was incremented stepwise within a predefined range. The drive field increment was set to 0.001 Oe. The zero crossings were registered within a 5000-ns period after waiting 2000 ns to be sure that all transients had ended. The calculations during each constant drive phase of this procedure were performed as for the stationary state.

IV. SYMBOLIC DYNAMICS AND SEQUENTIAL ORDER PARAMETER

To calculate algorithmic complexity as the sequential order parameter the following procedure was applied.

The one-dimensional time series to be analyzed was embedded in an m-dimensional delay coordinate space with the use of the Takens theorem [29]. Next, the following method of symbolic coding was used: (i) define a time window containing a fixed number of points N, (ii) for the given time window calculate an average a_k, where $k=1,\ldots,m$ is the index of the delay coordinate, and (iii) within the time window, associate an m-dimensional vector consisting of the symbols $C_k(t)$ with each point of the delay coordinate space trajectory:

$$C_k(t)=0 \quad \text{if } x[t+(k-1)\tau]\leqslant a_k-\varepsilon,$$

$$C_k(t)=1 \quad \text{if } a_k-\varepsilon<x[t+(k-1)\tau]<a_k+\varepsilon,$$

$$C_k(t)=2 \quad \text{if } x[t+(k-1)\tau]\geqslant a_k-\varepsilon$$

$$\text{for } k=1,2,\ldots,m,$$

where x is the signal analyzed, t is the index of the time series (integer time), and τ is the Takens delay.

For one-dimensional maps, the choice of the number of symbols used is typically related to the number of critical points of the map [4] but in our case such an analysis is impossible for the return maps obtained for the domain wall are extremely complex, higher-order sets. Moreover, the coding threshold ε for each control parameter value would have to be determined separately, which would make the analysis too complicated. In any case, it may seem at first glance that two symbols would be enough to code a time series obtained numerically. We found it necessary to add the middle symbol ''1'' to avoid the artifacts due to the error in the deter-

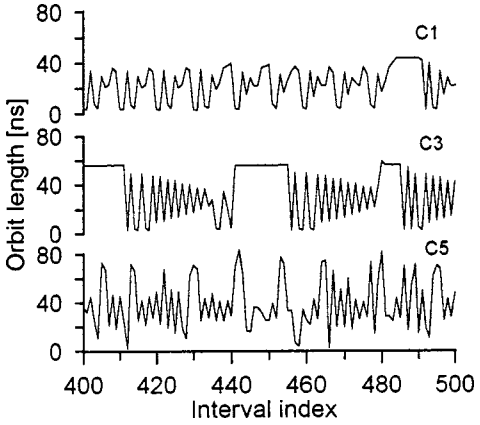

FIG. 2. Series of time intervals t_φ for the chaotic states $C1$, $C3$, and $C5$.

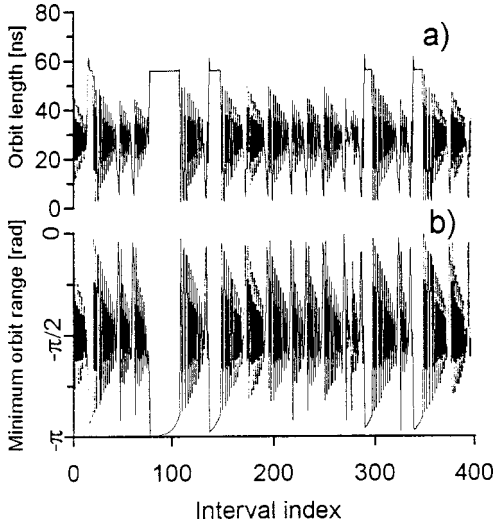

FIG. 3. The time intervals t_φ (curve *a*) and the corresponding extrema φ_s (curve *b*) for the chaotic state $C3$.

mination of the length of the orbit. The value of ε was set to 0.1, which is twice the numerical time step.

Each point in the m-dimensional delay coordinate space was thus represented by a single point in the corresponding m-dimensional coding space, i.e., by a symbolic word of m letters. After coding all the points in a time window, the algorithmic complexity was computed with each word of m symbols treated as a single element in the algorithm.

Algorithmic complexity counts the number of words that a string of length L may be decomposed into. The procedure introduced first by Lempel and Ziv is the following [10]. The word w_0 is the first symbol in the string. The word w_{k+1} is the shortest word following w_k that cannot be decomposed into $w_0, w_1, \ldots, w_k$. Formally algorithmic complexity is defined in the limit of $L \to \infty$.

We use algorithmic complexity as a local measure by computing its estimator in a short moving window containing a fixed number of data [6,8,30]. As the window is moved, a time series of the estimator is produced. The properties of the state analyzed are described by the properties of the probability distribution of the estimator of algorithmic complexity: the mean value, the position of maximum of the distribution, the minimum and maximum value of the estimator, etc. This kind of approach has already been successfully used for nonstationary systems [6,8,9]. In most of our calculations, we used the window length N equal to 100 but the values of: 10, 20, 50, 100, 200, and 500 were also studied.

Algorithmic complexity vanishes for periodic signals [10]. The estimator of algorithmic complexity has low values for periodic motion whereas for chaotic motion it typically does not exceed about one half of the window length. The moving average and the variance were also calculated for the same window length for comparison.

V. RESULTS

A. Time intervals of chaotic states

Figure 2 depicts examples of the dependence of the time intervals between zero crossings t_φ on the time for the chaotic states $C1$, $C3$, and $C5$, respectively. State $C1$ is chaotic despite the patterns visible in Fig. 2. State $C3$ containing the laminar regions not present in states $C1$ and $C5$ may be identified from Fig. 2 as intermittent. A separate study of the properties of this state is in preparation. States $C1$ and $C5$ seem more chaotic than $C3$ although the nature of these states seems to be different.

Figure 3 depicts the time dependence of the extrema (curve *b*) and the corresponding time intervals between crossings (curve *a*) for state $C3$. In the laminar regions the orbits have the same length but also have their minima at the same point, i.e., at the local minimum of energy in the vicinity of $\varphi = -\pi$ in the moving frame. During the turbulent phase, the trajectories oscillate around the local maximum of energy at $\varphi = -\pi/2$. One must remember that the system is spatially extended so that it tends towards a global minimum of energy. Thus it is not necessary that the value of the azimuthal angle φ at the midpoint of the Bloch wall have the orientation of the minimum of energy. It may be seen that the local minima, although unstable, still possess some attracting properties. A more detailed discussion of the problem of the local and global minima of energy requiring the examination of the system in space variables is in preparation.

For chaotic states the relation between t_φ and φ_s is not trivial. The laminar phases for the intermittent states like $C3$ are synchronized in both variables (they begin and end at the same time) but we found that the map $t_\varphi = t_\varphi(\varphi_s)$ is extremely complex. Note also that during the laminar phases the intercrossing intervals stay almost constant while the extrema of the variables drift (Fig. 3).

Figure 4 depicts the natural measures constructed from the time series of 5000 data points for states $C1$, $C3$, and $C5$. The well discernible peaks in the distribution for state $C3$ in this figure correspond to the two characteristic lengths of frequently visited orbits visible in Fig. 3. The right peak corresponds to the orbits ending near $\varphi = -\pi$ that are present during the laminar phase, whereas the left peak corresponds to those ending near $\varphi = 0$. Both of the peaks of the distribution are located in the vicinity of the equivalent local minima of energy. The shape of the distribution for $C3$ indicates a symmetry breaking effect while the two peaks obtained for $C1$ are symmetric. For state $C5$ the natural mea-

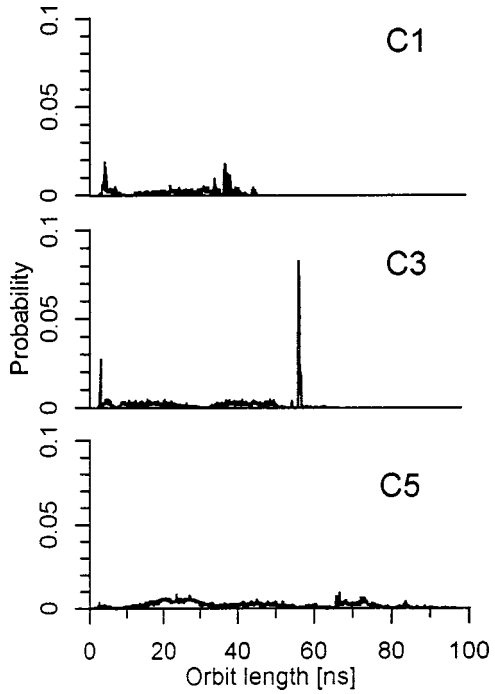

FIG. 4. Natural measure of the time intervals t_φ for the chaotic states $C1$, $C3$, and $C5$.

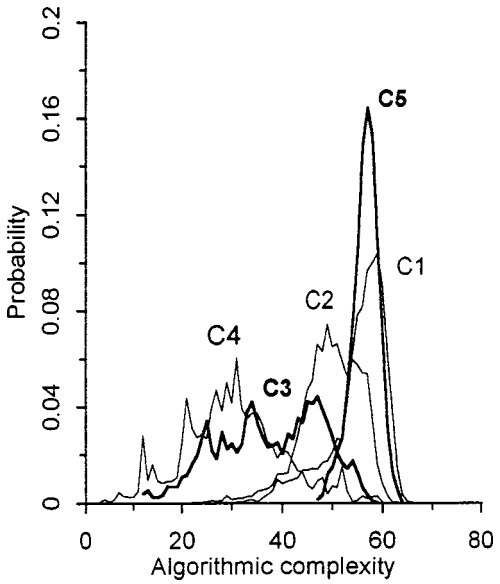

FIG. 5. Probability distributions of the algorithmic complexity C for the chaotic states. Note the different shape of histograms for the intermittent states $C3$ and $C4$.

sure contains no high peaks, which means that in this state there are no orbits of preferred length.

Above we have seen that the different states of the Bloch wall studied here certainly exhibit a different level of complexity. State $C3$ contains the most laminar regions and is thus less complex than the other chaotic states presented. It is interesting that although the states for smaller wall height h also contain only two Bloch lines their complexity is higher. The states for larger h contain more Bloch lines [16,18] and their complexity increases with an increasing thickness of the film, as will be shown below.

B. Choice of variable and method of data reduction

Due to the effect of the repeller situated in phase space at (0,0) (around which the trajectory spirals [16,18]) the time evolution of the series derived from the azimuthal angle $\varphi(z,t)$ are somewhat more complicated than those for $q(z,t)$. Although the time series of t_φ were used here for the algorithmic complexity calculations, the results for the time series of the maxima φ_s and the corresponding time series for variable $q(z,t)$ made for comparison were very similar. Due to the coarse graining of the symbolic coding procedures used here, the choice of the variable of the system was found to have no effect on the assessment of the relative level of complexity of chaotic states $C1-C5$. In intermittent states such as $C3$ and $C4$ the intercrossing intervals seem to be better suited for the analysis of the chaotic state because during the laminar phases, they remain almost constant while the extrema of the variables drift (Fig. 3).

C. Complexity of chaotic states

The results of algorithmic complexity calculations for states $C1-C5$ are depicted in Figs. 5 and 6. In Fig. 5 one may see that the shape of distributions of this measure is not

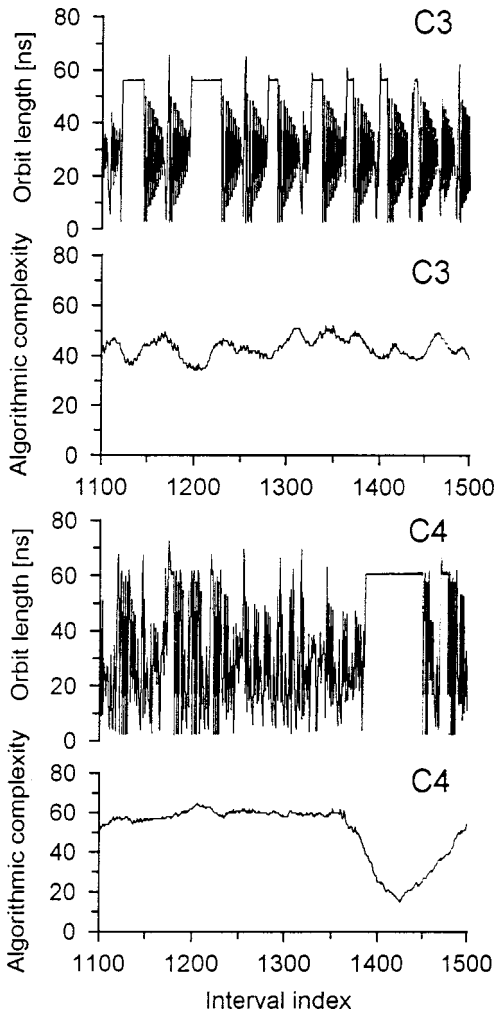

FIG. 6. Algorithmic complexity and the variable t_φ for states $C3$ and $C4$.

uniform. The distributions $C1$,$C5$, and to some extent $C2$, seem to form a family of reversed Poisson-like distributions. Such a shape of the distribution of the local order parameter was observed and is typical for the chaotic states [8,9,30]. State $C3$ has a dominantly bimodal distribution whereas state $C4$ has a wide Poisson-like distribution of the algorithmic complexity. Analyzing the distributions of algorithmic complexity we may conclude the following.

(a) The type of chaotic behavior for state $C1$ is different than for state $C2$. Indeed, earlier investigations showed that there is a periodic state in the region in between states $C1$ and $C2$ [17], which may result in a change of the type of chaotic behavior.

(b) The broad distributions for states $C3$ and $C4$ clearly indicate intermittency: these states are mixtures of phases with different levels of complexity. The distribution for $C4$ is the only one which is Poisson-like with the maximum at the left.

(c) The type of chaotic behavior for state $C5$ and the states for even higher values of the wall height is such that they are more chaotic than the other states. From earlier investigation we know that at these values of wall height the generation of a large number of Bloch lines occurs and their number increases with the height of the wall h [17,18]. It is interesting that state $C1$, which contains only two Bloch lines, has a similar average complexity. Note, however, that the distributions for $C1$ and $C5$ have a very different shape with the tail for $C1$ extending towards very low complexity levels.

The average or the position of the maximum of the histogram may be taken as the quantitative order parameter. If we analyze the position of the maximum, we may see that state $C4$ is the most ordered whereas $C1$ or $C5$ are the least. For intermittent states when the distribution is nonunimodal because the signal consists of two different phases, such an order parameter will show some change when the control parameter is varied but the determination of the true character of the state requires a further analysis of the shape of the distribution.

If just the time interval time series is analyzed, the relation between states $C3$ and $C4$ seems unclear (Fig. 6). State $C3$ seems to be apparently more ordered than $C4$ and has easy to distinguish periods of laminar and turbulent phase. On the other hand, one should keep in mind that the estimator of the algorithmic complexity is calculated in a time window of a fixed length (100). The finite time window introduces a time scale into the observation. As can be seen from the dominant magnitude of the algorithmic complexity in Fig. 6, state $C4$ is otherwise less ordered than $C3$. However, the lengths of the laminar phases are of the order of the window length, causing the complexity to decrease for brief periods of the time. This shifts the maximum of the distribution to the left. Thus, the local measures such as algorithmic complexity do exhibit fluctuations but the latter are in fact related to the local properties of the signal studied. If the window length chosen for the calculations were an order of magnitude smaller, the complexity of state $C3$ would be lower than the complexity of state $C4$. To conclude, the choice of the window length N is in fact the choice of the minimum time scale of a signal to which the local measure is to be sensitive to.

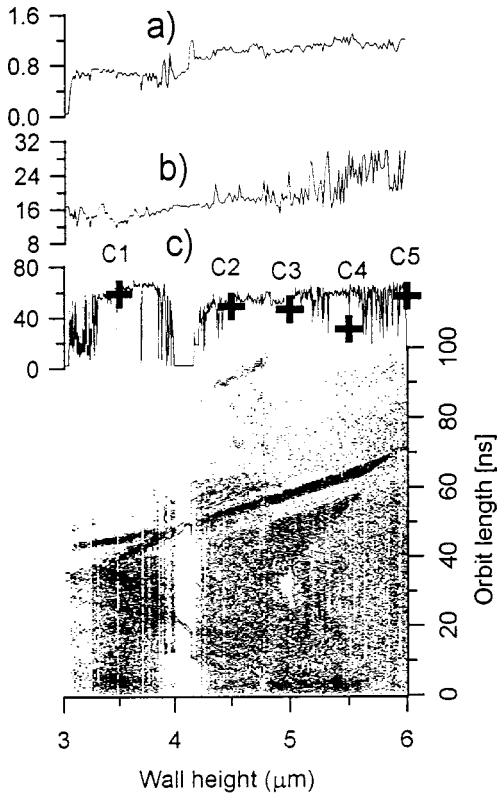

FIG. 7. Moving variance (curve *a*), moving average (curve *b*), and algorithmic complexity (curve *c*) as a function of the wall height every 0.005 μm. Bifurcation diagram depicted by dots. Algorithmic complexity of the chaotic states $C1-C5$ studied in [14–17] denoted by crosses.

When the method of time intervals was used it became possible to identify states $C3$ and $C4$ as intermittent by simply looking at the behavior of the intervals with the time (Fig. 2). There are, however, certain situations when such qualitative distinction is not enough because it says nothing about the relative order of two given states. The idea of characterizing complexity of different states of the dynamical system by single values of the order parameter is useful when we have to analyze the system behavior in a wide range of parameters to discern regions of different dynamics. The systems for which such an approach will be even more constructive are nonstationary systems with nonquasistatic parameter changes, as biological systems, where we have to monitor a system subject to unknown changes of the parameters.

The results of the calculation of algorithmic complexity obtained when the wall height was changed with the small increment of 0.005 μm are depicted in Fig. 7 together with the bifurcation diagram, which was formed by plotting all the attractor orbit lengths corresponding to each wall height in a separate vertical line. The algorithmic complexity plot (curve *c*) is accompanied by the moving average (curve *b*) and the moving variance (curve *a*) calculated in the sliding time window of the same length equal to 100. It can be seen that regions of intermittent or periodic behavior in which the values of algorithmic complexity are lower are frequent in parameter space. States $C3$ and $C4$ are located in such regions. There is no visible effect of the characteristic length of the system (the soliton width 0.3 μm) on the level of

complexity as the wall height is varied.

The moving average as well as the variance are not suitable as quantitative measures of complexity. This is particularly well visible for the periodic window at around $h = 4.0\,\mu$m, which was not detected by either of them. These quantities do not describe the nonlinear dynamics of the system. Note that in certain parameter ranges of the control parameter in Fig. 7, a number of periodic windows can be easily identified by the downward spikes of the algorithmic complexity that are not always visible in the bifurcation diagram. Note also that the algorithmic complexity is much easier to calculate automatically than any fractal dimension so that we could relatively easily perform the calculations for 500 states, as depicted in Fig. 7, on a standard PC.

D. The choice of parameters of the embedding

The probability distributions of algorithmic complexity for all chaotic states $C1-C5$ were calculated with the value of the delay τ varied from 1 to 20 and for embedding dimensions from 1 to 5. The relative properties of the distributions of algorithmic complexity for the different chaotic states remained unchanged for a relatively wide range of embedding dimensions and delay times. We consider the embedding dimension $m=4$ or $m=5$ optimal for the purpose of the assessment of the relative complexity of the chaotic states. For $m=1$ the shape of the distributions does not change with the control parameter. The nature of the signal may not be ascertained as the differences in positions of the distributions are of the order of 5%. On the other hand, the increase of the embedding dimension above $m=5$ leads to very complex shapes of the distributions of algorithmic complexity. Furthermore, an embedding dimension between 4 and 5 agrees very well with the calculations of the fractal dimensions for the chaotic states of the Bloch wall where it was found that the correlation dimension does not exceed 2.5 [11,12]. We found the optimal delay to be $\tau=4$ because for this value all the typical features of algorithmic complexity distributions are clearly visible. Finally we have used $\tau=4$ and $m=5$ as the optimal reconstruction parameters. Embedding a one-dimensional signal using the Takens theorem combined with the m-dimensional symbolic coding enables us to achieve more sensitivity.

E. Nonstationary data

The results of the analysis of the artificially created nonstationary data is depicted in Fig. 8. The segments of data from states $C1$ and $C3$ normalized as to have the same mean and variance are alternating as shown by the rectangular curve. The topmost curve (curve *a*) shows the data whereas curves *b* and *c* show the algorithmic complexity calculated for the time window length 100 and 10, respectively. The dashed lines in Fig. 8 mark the levels of complexity for states $C1$ and $C3$.

It may be seen that algorithmic complexity detects the changes of state even if the mean and the variance do not change from one segment to the other significantly. Note that the magnitude of algorithmic complexity of the normalized signal is the same as in Fig. 5 (distribution maxima) for the nonnormalized data. For the window of length 100 the difference in complexity between the states is of the order of

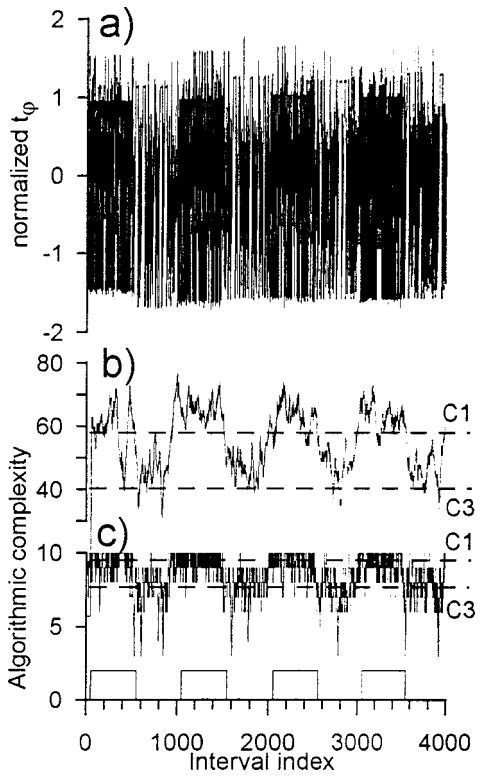

FIG. 8. Artificial nonstationary signal (curve *a*) and algorithmic complexity for window length $N=100$ (curve *b*) and for $N=10$ (curve *c*). Moments of switching marked below by the square wave. Average algorithmic complexity for $C1$ and $C3$ is marked by dashed horizontal lines.

50%. The above result may be obtained only if the observation window is shorter than the mean value of the length of the phases of different states (in this case the length of such phases is 500). This is a clear advantage of the estimator of algorithmic complexity calculated as a local measure over the same quantity calculated from the definition, i.e., including the limit to infinity. In this limit, the identification of phases of different states would be impossible.

The length of the observation window may be made even shorter than 100, which enables us to detect better the very moment of phase switching, not only its presence. Note that even for the extreme value of window length $N=10$ (curve *b*) the moment of switching is detected although both states are not as clearly discerned as in case of the window length $N=100$ (curve *c*). For the curves *b* and *c* the value of the coding parameter ε was set to 0.001, which enhanced the sensitivity. This indicates that for the detection of the moment of switching, two-symbol coding is better than three-symbol coding. In general, the value of ε should exceed the noise level in the system studied no matter what the source of the noise. The noise may be external but it also may be a property of the measurement (e.g., the error of the estimation of the orbit length). Neglecting this requirement causes misleading effects obtained for the periodic states. On the other hand, this parameter should be as low as possible, otherwise some details in the signal relevant to the dynamics would be ignored.

The results for the nonstationary slowly varying drive field are the following. The bifurcation diagram and the algorithmic complexity curve are depicted in Fig. 9 together

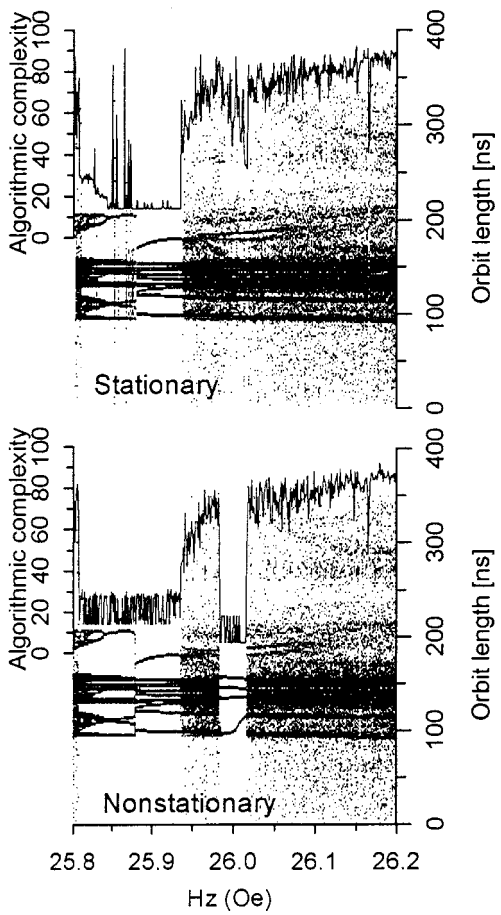

FIG. 9. Fragment of the bifurcation diagram as a function of the magnitude of the drive field for the constant wall height $h = 1.1\ \mu$m and the resultant algorithmic complexity curve for the stationary and nonstationary changes in the drive field.

with the results for stationary calculations in the same range added for comparison. It may be seen that for the nonstationary case, there exists a periodic solution at about 26 Oe visible in the stationary case only as a narrow window. This periodic state in the nonstationary case is sensitive to the history of evolution of the system. For a different scenario of the drive field increments and different lengths of the step this effect may not occur in this range of the drive field. However, it was observed frequently during the calculations for various nonstationarity scenarios. The effect discussed here seems to be the equivalent to tracking observed until now in maps [31]. In this phenomenon the stability range of the periodic orbit may be extended by applying small changes of the system parameter. The phenomenon observed in the domain wall under a slowly varying drive seems to be a ''self-tracking'' effect as no external stochastic or chaos control algorithm perturbations were applied in our case. It is probable that multistability plays a role in this effect.

Algorithmic complexity within the stability range of periodic solutions fluctuates in a nonstationary case. These fluctuations are the direct consequence of fluctuations in the lengths of the orbit that are of the order of 0.5 ns (10 time steps), which are not visible in the bifurcation diagram due to the scale used. Note that there are no such fluctuations at the right end of the stability range of the new periodic solution. Also, there is a drop in the complexity at 26 Oe in the stationary case, which indicates a narrow periodic window. Nonstationarity stabilizes and extends the stability range of this window.

VI. CONCLUSIONS

The chaotic states of a complex system—the model of a magnetic domain wall—were analyzed. We applied a multidimensional form of symbolic dynamics to an m-dimensional delay coordinate reconstruction of the trajectory of the system. A local measure: a short window estimator of the algorithmic complexity of the series of words obtained from the symbolic coding was used as the sequential order parameter and compared with the mean and the variance calculated in a sliding window.

We demonstrated that this method is suitable for the characterization of states of different complexity, especially if the system behavior is to be analyzed in a wide range of the control parameter. It is also suitable for the detection of intermittency and chaos-chaos intermittency because the method allows us to identify phases of different dynamics in a signal, even when there is no difference in the mean and the variance, and has the ability to detect precisely the moments of switching between different phases in the signal. This last property makes the method suitable for the analysis of nonstationary systems with step-wise changes of the control parameter. Altering the window length enables us to choose the minimum time scale to which the order parameter will be sensitive. Such a characterization seems to yield more information than a fractal analysis applied earlier to the same chaotic states [11,12] and certainly is better able to discern the different states of the system.

For nonstationary changes of the drive field we observed the extension of the stability of the periodic solution onto a wider parameter range. This phenomenon may be similar to tracking in simple maps [31].

ACKNOWLEDGMENT

This work was supported financially by the KBN Grant No. 2P03B 020 09.

[1] E. Ott, *Chaos in Dynamical Systems* (Cambridge University Press, New York, 1993).

[2] M. Casdagli, Physica D **108**, 12 (1997); J. P. Eckmann and D. Ruelle, Rev. Mod. Phys. **57**, 617 (1985).

[3] C. Amitrano and R. S. Berry, Phys. Rev. Lett. **68**, 729 (1992).

[4] B-L. Hao, *Elementary Symbolic Dynamics and Chaos in Dissipative Systems* (World Scientific Publishing, Singapore, 1989).

[5] A. Voss, J. Kurths, H. J. Kleiner, A. Witt, N. Wessel, P. Saparin, KJ. Osterziel, R. Schurath, and R. Dietz, Cardiovasc. Res. **31**, 419 (1996).

[6] J. J. Żebrowski, W. Popławska, R. Baranowski, and T. Buch-

ner, J. Tech. Phys. **38**, 415 (1997).
[7] A. Witt, J. Kurths, F. Krause, and K. Fischer, Geophys. Astrophys. Fluid Dyn. **77**, 79 (1994).
[8] J. J. Żebrowski, W. Popławska, R. Baranowski, and T. Buchner, Chaos Solitons Fractals (to be published).
[9] J. J. Żebrowski, W. Popławska, R. Baranowski, and T. Buchner, Acta Phys. Pol. B (to be published).
[10] A. Lempel and J. Ziv, IEEE Trans. Inf. Theory **IT-22**, 75 (1976); F. Kaspar and H. G. Schuster, Phys. Rev. A **36**, 842 (1987).
[11] M. Wierzbicki and J. J. Żebrowski, Acta Phys. Pol. B **27**, 2045 (1996).
[12] J. Żebrowski, Phys. Rev. E **47**, 2308 (1993).
[13] A. Sukiennicki and R. A. Kosiński, Chaos, Solitons and Fractals **9**, 181 (1998).
[14] R. A. Kosiński and A. Sukiennicki, Acta Phys. Pol. A **89**, 495 (1996).
[15] J. J. Żebrowski and A. Sukiennicki, in *Deformations of Mathematical Structures II: Surface Effects*, edited by J. Ławrynowicz (Kluwer, Netherlands, 1994), pp. 435–460.
[16] J. Żebrowski and A. Sukiennicki, Acta Phys. Pol. B **24**, 785 (1993).
[17] J. J. Żebrowski, Phys. Rev. B **39**, 7205 (1989).
[18] J. J. Żebrowski, Phys. Scr. **38**, 632 (1988).
[19] N. L. Schryer and L. R. Walker, J. Appl. Phys. **45**, 5406 (1974).
[20] J. J. Żebrowski and A. Sukiennicki, Proc. SPIE **2037**, 290 (1994).
[21] J. J. Żebrowski and A. Sukiennicki, J. Magn. Magn. Mater. **140-144**, 2001 (1995).
[22] R. Castro and T. Sauer, Phys. Rev. E **55**, 287 (1997).
[23] R. Hegger and H. Kantz, Europhys. Lett. **38**, 267 (1997).
[24] L. Glass, P. Hunter, and A. McCulloch, *Theory of Heart* (Springer, New York, 1991).
[25] M. A. Woo, W. G. Stevenson, D. K. Moser, R. B. Trelease, and R. M. Harper, Am. Heart J. **123**, 704 (1992).
[26] A. Namajunas and A. Tamasevicius, Physica D **58**, 482 (1992).
[27] E. N. Lorenz, J. Atmos. Sci. **20**, 130 (1963).
[28] J. Becker, F. Rödelsperger, Th. Weyrauch, H. Benner, and A. Cenys, Phys. Rev. E **59**, 1622 (1999).
[29] F. Takens, Phys. Rev. Lett. **51**, 1265 (1980).
[30] T. Buchner and J. J. Żebrowski, Chaos, Solitons and Fractals **9**, 19 (1997).
[31] I. Triandaf and I. Schwartz, Phys. Rev. E **48**, 718 (1993).